

FDTD Analysis of Platform Effect Reduction with Thin Film Ferrite

Zhi Yao, Qiang Xu and Yuanxun Ethan Wang

Electrical Engineering Department, University of California, Los Angeles, CA, 90024, USA

Abstract — Conformal antennas suffer from the platform effect on which the radiation of the current become inefficient due to the existence of the image current in the opposite direction. The platform effect may be well shielded with thin film ferrimagnetic material that has a high in-plane permeability. A one-dimensional finite difference time domain method (1-D FDTD) is developed to model the current radiations off the thin-film ferrite coated ground plane. Both the ferromagnetic resonances (FMR) of the ferrite and the radiation of electromagnetic wave caused by the dynamic magnetic field are simulated, by solving Landau-Lifshitz-Gilbert (LLG) equation and Maxwell's equations simultaneously. The simulated relative permeability curve matches with the theoretical results. Radiated power is computed as well, which increases as the thickness of the film increases or the FMR line width of the material susceptibility decreases.

Index Terms — Electromagnetic radiation, ferrite films, ferroresonance, finite difference time domain methods, permeability.

I. INTRODUCTION

Traditional low profile conformal antennas suffer the platform effect, which is caused by the cancellation of the radiation of the image current and the original current source. The platform effect also indicates excessive storage of reactive energy within the antenna structure [1], [2]. Utilizing high permeability magnetic material to improve the radiation efficiency has been proposed and studied in [3]–[5]. The wide interest in using magnetic materials as the antenna substrate raises the necessity of physical insight into such type of materials. Various numerical computations are executed to model different structures composed of ferrite materials [6]–[8]. In this paper, a one-dimensional finite difference time domain method (1-D FDTD) is developed to model current radiations off the thin-film ferrite coated ground plane, which takes care of the dual-way interactions between the magnetization and electromagnetic field. The equation of motion of electron spin, also known as the Landau-Lifshitz-Gilbert (LLG) equation is coupled with Maxwell's equations to model the dispersive nature of the magnetization and the loss mechanism due to hysteresis. Both the ferromagnetic resonances (FMR) and radiation of electromagnetic wave caused by the dynamic magnetic field are simulated.

II. 1-D FDTD MODELING

Fig. 1 shows the thin-film ferrite antenna structure. The thickness of the film is $d = 1\mu m$. The dimension of the film is assumed to be infinitely large in the horizontal plane so that the 1-D approximation is valid. A static magnetic field bias H_i and a dynamic current excitation are applied in the y direction, so that dynamic magnetic field is generated in the x direction and the z direction. In Fig. 1, the term M_s is the saturation magnetization, \bar{m} is the additional (AC) magnetization caused by \bar{h} . This dynamic magnetization modeling will solve the Maxwell's equations and LLG equations simultaneously as both the magnetic moment and electromagnetic coupling phenomena exist physically and inseparably in the ferrite.

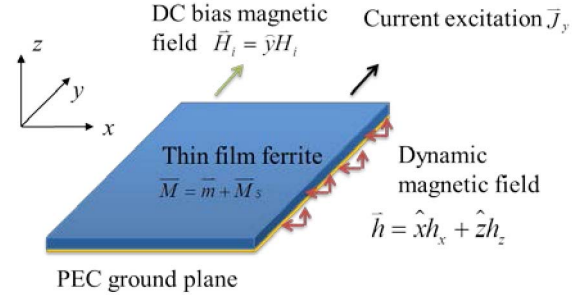


Fig. 1. Thin-film ferrite antenna structure.

The original vector form of the LLG and Maxwell's dynamic system is composed of the following equation set as in (1)–(2).

$$\frac{\partial \bar{M}}{\partial t} = \mu_0 \gamma (\bar{M} \times \bar{H}) - \frac{\alpha}{|\bar{M}|} \bar{M} \times \frac{\partial \bar{M}}{\partial t} \quad (1)$$

$$\frac{\partial \bar{E}}{\partial t} = \frac{1}{\epsilon_r \epsilon_0} \nabla \times \bar{H}, \quad \frac{\partial \bar{B}}{\partial t} = -\nabla \times \bar{E} \quad (2)$$

In (1), both gyromagnetic ratio γ and the damping factor α are negative. $\gamma = -1.759 \times 10^7 \text{ rad} / (s \cdot Oe)$. With the small signal approximation, (1) is expanded in the following scalar form [7]:

$$\frac{1}{\mu_0} \frac{\partial b_z}{\partial t} - \frac{\partial h_z}{\partial t} = \gamma [H_i b_x - \mu_0 (M_s + H_i) h_x] + \alpha \left[\frac{1}{\mu_0} \frac{\partial b_x}{\partial t} - \frac{\partial h_x}{\partial t} \right] \quad (3)$$

$$\frac{1}{\mu_0} \frac{\partial b_x}{\partial t} - \frac{\partial h_x}{\partial t} = \gamma [-H_i b_z + \mu_0 (M_s + H_i) h_z] - \alpha \left[\frac{1}{\mu_0} \frac{\partial b_z}{\partial t} - \frac{\partial h_z}{\partial t} \right] \quad (4)$$

$$b_y = \mu_0 h_y. \quad (5)$$

Enforcing 1-D approximation to (2) reduces the Maxwell's equations to

$$\frac{\partial b_x}{\partial t} = \frac{\partial e_y}{\partial z}, \quad e_z = 0, \quad b_z = 0 \quad (6)$$

which further simplifies (3) and (4) into

$$-\frac{\partial h_z}{\partial t} = \gamma [H_i b_x - \mu_0 (M_s + H_i) h_x] + \alpha \left[\frac{1}{\mu_0} \frac{\partial b_x}{\partial t} - \frac{\partial h_x}{\partial t} \right] \quad (7)$$

$$\frac{1}{\mu_0} \frac{\partial b_x}{\partial t} - \frac{\partial h_x}{\partial t} = \gamma [\mu_0 (M_s + H_i) h_z] + \alpha \frac{\partial h_z}{\partial t}. \quad (8)$$

In time domain numerical modeling, the stability condition between the spatial grid and the time step is $\max(\Delta x, \Delta y, \Delta z) \geq c\Delta t/\sqrt{3}$ to stabilize the iteration process. If the antenna works at 1 GHz, the ratio of the wavelength and the structure dimension is $\lambda/h = 3 \times 10^5$, thus even though the whole structure occupies only one spatial grid, the duration of one time step has to be no larger than $\Delta t_{\max} = 6 \times 10^{-15} s$. If a time window of $10^{-9} s$ should be simulated, the number of time steps is almost one million, which is enormous data. To avoid this stability problem, the following polynomial spatial expansion of electromagnetic field is used:

$$e_y = e_{y1} z, \quad h_x = h_{x0}, \quad b_x = b_{x0} \quad (9)$$

where e_{y1} , h_{x0} and b_{x0} are unknowns to be solved. With the spatial expansion, the stability issue is cleverly avoided, and the simulation will be much less time and storage consuming. Therefore, the radiation boundary condition

$$\left. \frac{E_y}{H_x} \right|_{z=d} = \eta_0 \quad (10)$$

yields

$$e_{y1} = -\frac{\eta_0}{d} (h_{x0} + J_y) \quad (11)$$

where J_y is the surface current excitation. Substituting (6) and (11) into (7) and (8) gives

$$\frac{\partial b_{x0}}{\partial t} = -\frac{\eta_0}{d} (h_{x0} + J_y) \quad (12)$$

$$-\frac{\partial h_z}{\partial t} = \gamma H_i b_{x0} - \gamma \mu_0 (M_s + H_i) h_{x0} - \frac{\alpha \eta_0}{d \mu_0} (h_{x0} + J_y) - \alpha \frac{\partial h_{x0}}{\partial t} \quad (13)$$

$$-\frac{\eta_0}{d \mu_0} (h_{x0} + J_y) - \frac{\partial h_{x0}}{\partial t} = \gamma \mu_0 (M_s + H_i) h_z + \alpha \frac{\partial h_z}{\partial t}. \quad (14)$$

The time difference equations are obtained by discretizing (12)–(14), as follows:

$$k_1 \cdot h_{x0}^n = k_2 \cdot h_{x0}^{n-1} - \left(\alpha + \frac{1}{\alpha} \right) \frac{\eta_0}{\mu_0 d} \frac{J_y^n + J_y^{n-1}}{2} - \frac{\gamma}{\alpha} (M_s + H_i) \mu_0 h_z^{n-\frac{1}{2}} + \gamma H_i b_{x0}^{n-\frac{1}{2}} \quad (15)$$

$$b_{x0}^{n+\frac{1}{2}} = -\frac{\eta_0 \Delta t}{d} [h_{x0}^n + J_y^n] + b_{x0}^{n-\frac{1}{2}} \quad (16)$$

$$k_3 \cdot h_z^{n+\frac{1}{2}} = k_4 \cdot h_z^{n-\frac{1}{2}} - \gamma H_i \frac{b_{x0}^{n+\frac{1}{2}} + b_{x0}^{n-\frac{1}{2}}}{2} + \gamma \mu_0 (M_s + H_i) h_{x0}^n \quad (17)$$

where

$$k_{1,2} = \left(\frac{\eta_0}{2\mu_0 d} + \frac{1}{\Delta t} \right) \left(\alpha + \frac{1}{\alpha} \right) \pm \frac{(M_s + H_i) \mu_0 \gamma}{2} \quad (18)$$

$$k_{3,4} = \frac{(\alpha^2 + 1)}{\Delta t} \pm \frac{\alpha \gamma \mu_0 (M_s + H_i)}{2}. \quad (19)$$

A surface electric current density in the form of Gaussian pulse $J_y = e^{-(t-t_0)^2/2\tau}$ is applied to the thin film, as the excitation to the recursive FDTD time-marching algorithm. The leap-frog time stepping scheme can be implemented by solving the aperture dynamic component h_{x0} , coupled back to update the magnetic flux density and then to update the other magnetic field component h_z . The ferrite material is chosen to be yttrium iron garnet (YIG), with $4\pi M_s = 1750 \text{ Gauss}$, $\Delta H = 5 \text{ Oe}$, $\varepsilon_r = 15$.

III. SIMULATION RESULTS

The relative permeability curves shown in Fig. 2 are obtained by the ratio of the frequency domain fields, which are computed using the fast Fourier transform of the time domain field. The analytical results are computed based on [9]:

$$\omega_0 = \mu_0 \gamma H_i + j\alpha\omega, \quad \chi = \frac{\omega_m(\omega_m + \omega_0)}{[\omega_0(\omega_m + \omega_0) - \omega^2]} \quad (20)$$

where ω_0 is the precession frequency, $\omega_0 = \mu_0 \gamma H_i$, and $\omega_m = \mu_0 \gamma M_s$. The FMR is shifted to higher frequencies as the DC magnetic bias increases. A very good agreement between the simulated results and the analytical results can be observed in Fig. 2. The normalized radiated power into free space (shown by Fig. 3) increases as the thickness of the film increases or the line width of the material decreases. It should be noted that the radiated power is maximum at FMR, where the magnetic loss

tangent reaches its peak and the relative permeability is nearly zero. This phenomenon was not predicted prior to this research. It can be explained that near FMR region, the ferrite becomes a good magnetic conductor so that dynamic electromagnetic fields could hardly stand inside the material, which results in high power released into the free space. This conclusion opens up a new antenna design strategy to make the antenna work at FMR to enhance the radiation.

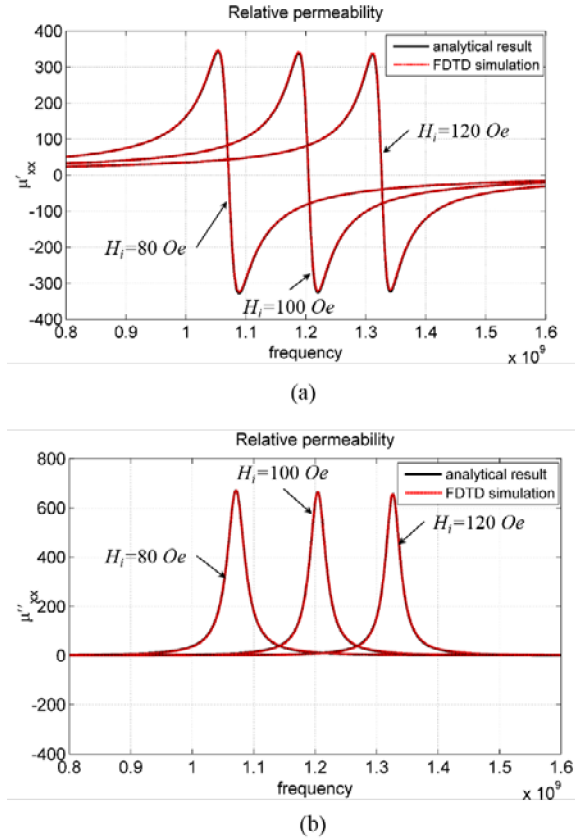


Fig. 2. Relative permeability with different DC magnetic bias, $\Delta H = 50 \text{ Oe}$. (a) Real part μ' . (b) Imaginary part μ'' .

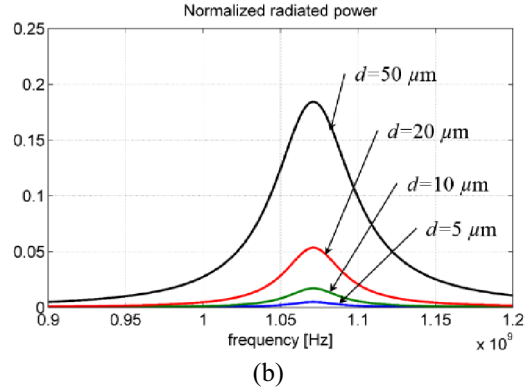
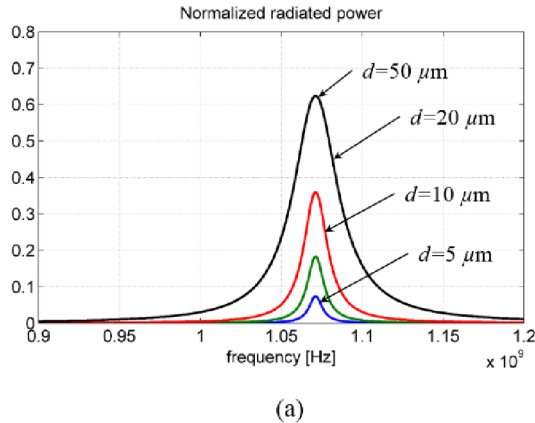


Fig. 3. Normalized radiated power of the thin film ferrite. (a) $\Delta H = 10 \text{ Oe}$, (b) $\Delta H = 50 \text{ Oe}$.

III. CONCLUSION

A thin film ferrite antenna is modeled by the 1-D FDTD technique, which simulates the bidirectional coupling effect of Maxwell's equations and LLG equation. The modeling is fully validated by the agreement between the simulated results and the theoretical solutions. The thin film ferrite antenna shows the potential of overcoming the platform effect by presenting decent radiation efficiency near FMR.

REFERENCES

- [1] J. C.-E. Sten, A. Hujanen, and P. K. Koivisto, "Quality factor of an electrically small antenna radiating close to a conducting plane," *IEEE Trans. Antennas Propag.*, vol. 49, no. 5, pp. 829–837, May 2001.
- [2] Z. Yao and Y. Wang, "Dynamic analysis of acoustic wave mediated multiferroic radiation via FDTD methods," *2014 IEEE Int. Symp. on Antennas and Propag.*, Memphis, USA, Jul. 6–11, 2014.
- [3] R. C. Hansen and M. Burke, "Antennas with magneto-dielectrics," *Microw. Opt. Technol. Lett.*, vol. 2, pp. 75–78, 2000.
- [4] H. Mosallaei and K. Sarabandi, "Magneto-dielectrics in electromagnetics: concept and applications," *IEEE Trans. Antennas Propag.*, vol. 52, no. 6, pp. 1558, 1567, Jun. 2004.
- [5] P. M. T. Ikonen, K. N. Rozanov, A. V. Osipov, P. Alitalo, and S. A. Tretyakov, "Magnetodielectric substrates in antenna miniaturization: potential and limitations," *IEEE Trans. Antennas Propag.*, vol. 54, no. 11, pp. 3391, 3399, Nov. 2006.
- [6] O. Vacus and N. Vukadinovic, "Dynamic susceptibility computations for thin magnetic films," *J. of Comput. and Appl. Math.*, vol. 176, no. 2, pp. 263–281, Apr. 2005.
- [7] J. A. Pereda, L. A. Vielva, M. A. Solano, A. Vegas and A. Prieto, "FDTD analysis of magnetized ferrites: application to the calculation of dispersion characteristics of ferrite-loaded waveguides," *IEEE Trans. Microw. Theory Techn.*, vol. 43, no. 2, pp. 350–357, 1995.
- [8] L. Bañas, "Adaptive techniques for Landau–Lifshitz–Gilbert equation with magnetostriction," *J. of Comput. and Appl. Math.*, vol. 215, no. 2, pp. 3047–310, Jun. 2008.
- [9] D. M. Pozar, *Microwave Engineering*, JohnWiley & Sons, Inc., 2012.